THE SIMULATION OF FUEL CELL COGENERATION SYSTEMS WITHIN RESIDENTIAL BUILDINGS

Ian Beausoleil-Morrison [1], Dave Cuthbert [2]
Gord Deuchars [3], Gordon McAlary [3]

[1] CANMET Energy Technology Centre, Natural Resources Canada, Ottawa (ibeausol@nrcan.gc.ca)
[2] Kinectrics Inc, Toronto (Dave.Cuthbert@kinectrics.com)
[3] Fuel Cell Technologies Ltd, Kingston, Ontario (gord@fuelcelltechnologies.ca / gmcalary@fct.ca)

ABSTRACT

A fuel cell (FC) model was developed within the ESP-r/HOT3000 program to enable the simulation of residential buildings serviced by FC-cogeneration systems. Empirical relations in parametric form are used to represent the fuel cell's thermal and electrical performance. This approach is well suited to the current state and rapid pace of fuel cell development as the model makes direct use of benchmark test results. The new model is demonstrated by simulating a modern energy-efficient house serviced by an internally reforming solid-oxide fuel cell (SOFC) cogeneration system. Although these results are specific to the case simulated, the model does demonstrate that SOFC-cogeneration systems have the potential for delivering high system efficiencies in residential buildings.

INTRODUCTION

There has been significant interest in recent years in distributed generation (DG) technologies such as photovoltaics, wind turbines, micro-turbines, and reciprocating engines. Utility restructuring, concerns over reliability of supply, and the potential for improved efficiency are some of the driving factors for locating these small (a few kW to a few MW) electrical power systems close to the point of electrical consumption.

Fuel cells (FC) are an interesting technology for residential-building scale DG because they offer the potential for cogeneration—the concurrent production of electrical and thermal energy. Fuel cells are energy conversion devices that convert chemical energy directly into electrical energy. This is accomplished through the electrochemical oxidation of a fuel (hydrogen) and the electrochemical reduction of oxygen. These electrochemical reactions occur at electrodes which are continuously fed with hydrogen and oxygen and which are separated by an electrolyte layer.

A solid oxide fuel cell (SOFC) cogeneration system for residential buildings is currently under development at Fuel Cell Technologies Ltd (FCT). SOFCs, which use a solid metal oxide as the electrolyte, show particular promise for residential cogeneration applications because of their high operating temperature (600 to 1 000^oC). These temperatures are sufficient to internally reform hydrogen from natural gas. This means that the fuel cell can be supplied with natural gas, which is readily available in many residential buildings. The gas' constituent hydrocarbon molecules (methane, ethane, propane, etc.) are reformed to hydrogen at a catalyst within the fuel cell, and the hydrogen then supplied to the electrode. Internal reforming avoids either the need to deliver and store hydrogen at the building site, or the cost, energy, and space requirements of an external fuel reformer. The second advantage of the SOFC's high operating temperature is the production of thermal energy at temperatures that can be exploited for space and domestic water (DHW) heating. The interested reader is referred to US-DOE (2000) for a overview of SOFC and other fuel cell technologies and to Ellis and Gunes (2002) for a discussion on the use of fuel cells for building cogeneration.

The FCT SOFC-cogeneration system consists of: an internally reforming SOFC; systems to supply air and natural gas to the SOFC; a power conditioning system to convert the electrical power from direct to alternating current; and a heat exchanger to extract thermal energy from the hot exhaust gases to supply the house's thermal requirements. As the SOFC will convert 40% to 50% of the fuel's chemical energy (based on the lower heating value, LHV) to electrical energy, the effective exploitation of the thermal output is critical to realizing high total efficiencies. Simulation represents a powerful and flexible technology for studying and optimizing this complex thermodynamic system. Interactions between the SOFC-cogeneration system and a house's thermal and electrical demands can be analyzed, and the impact of design variables such as the configuration of the balance of the HVAC plant, thermal storage capacity, and component efficiencies can be examined.

This provided the motivation for developing FC-cogeneration modelling capabilities within the ESP-r/HOT3000 building simulation engine. The research

objectives were to produce a comprehensive simulation tool that could accurately model the thermal performance of residential buildings serviced by FC-cogeneration systems. Although the immediate interest was SOFCs, the model was structured in a generic fashion to also enable the simulation of proton exchange membrane (PEM), phosphoric acid, and other fuel cell technologies. The resulting model is useful for analyzing the technical and economic potential of FC-cogeneration systems and for assessing system design variants.

To begin, this paper provides a brief overview of the ESP-r/HOT3000 simulation engine. Following this, the fuel cell model is presented in detail. Application of the new model is then demonstrated by simulating a modern energy-efficient house serviced by an SOFC-cogeneration system. Finally, conclusions are drawn and recommendations made for further work.

ESP-r/HOT3000 SIMULATION ENGINE

The ESP-r/HOT3000 simulation engine is used as the platform for this work. This simulator is based upon the comprehensive and extensively validated ESP-r program developed at the University of Strathclyde (ESRU 2000), with algorithmic additions by the CANMET Energy Technology Centre (CETC) to support the modelling of Canadian (and international) housing. This section briefly summarizes ESP-r/HOT3000's simulation methodology.

Partitioned solution approach

While most building analysis tools exclusively simulate thermal processes, ESP-r/HOT3000, in contrast, strives to model all relevant physical processes in an integrated and rigorous fashion. The following modelling domains are treated: building thermal; inter-zone air flow; intra-zone air flow; heat, air, water, and moisture flow within the HVAC system; electric power flow; and illumination.

ESP-r/HOT3000 employs a partitioned solution approach, applying customized solvers to each model domain. This enables an optimized treatment of each of the disparate equation sets. In this manner, one solver processes the building thermal domain, another treats the HVAC domain, while yet another handles network air flow (to resolve inter-zone flow). Interdependencies are handled by passing information (handshaking) between the solution domains on a time-step basis, this allowing the global solution to evolve in a coupled manner (Clarke 2001b).

Building thermal domain

ESP-r/HOT3000 simulates the thermal state of the building using a control-volume heat-balance methodology, which is elaborated in detail by Clarke (2001a). This encompasses three principle steps. The building is discretized by representing rooms and fabric components (walls, windows, roofs, floors) with control volumes. A heat balance considering the relevant energy flow paths (convection, radiation, infiltration, ground heat transfer, etc.) is written for each control volume. A simultaneous solution is performed on the equation set to predict the thermal state of each control volume and the heat flows between control volumes for a given point in time. This process is repeated for each time-step of the simulation.

Explicit HVAC domain

ESP-r/HOT3000's explicit HVAC modelling domain is based upon a component-level approach whereby users assemble components into a coherent HVAC system. Data must be provided to define each component (e.g. a boiler) and the arrangement of the components. Users must also specify how components are controlled, indicating what variables are sensed (e.g. air temperature in a room), and how components are actuated (e.g. water flow through a coil) in response to the sensor signals.

Each component in the HVAC network is represented by one of more control volumes and each control volume is characterized by mathematical models that describe the control volume's energy and mass exchanges with connected components and the environment. The energy balances are expressed in the following form,

$$(Mc_p)\frac{\partial T}{\partial t} = \sum_{i=1}^{i=n} q_i \qquad (1)$$

Where M is the mass of the control volume, c_p its heat capacity, T its temperature, t is time, and q_i is an energy flow into the control volume.

The left side of this equation represents the rate of change of energy storage in the control volume. The right side represents all the energy flows which affect the control volume's thermal state. Depending upon the component under consideration, these energy flows might be a convective flux from the skin of the component to the containing room, an energy release due to combustion, or advection resulting from water or air flow through the control volume. These energy flows can be expressed with simple or complex models and can be based upon first-principle or empirical approaches, as the situation dictates. Similar equations are written to represent the water and air mass balances on each control volume.

Writing energy and mass balances for each control volume leads to the formation of three matrices of equations that describe the HVAC plant network's thermal and mass flow state. A direct solution

approach is used to solve these three matrices. As the equation set is highly non-linear, iteration is used to reform and resolve the matrices until convergence is achieved (refer to Hensen 1991 for details).

The simulation of the building thermal and HVAC domains evolves by handshaking solution variables between the domains each time-step. For example, the building thermal domain's room air temperature solution is passed to the HVAC domain. These data are used to calculate containment losses in the energy balances for certain HVAC components (e.g. a boiler) and for controlling components in the HVAC plant network. The energy injected to rooms by the HVAC system is then communicated to the building thermal domain where it is used in the formation and solution of the energy balances for the rooms. This process is repeated each time-step of the simulation.

FUEL CELL MODEL

This section describes the component model developed for ESP-r/HOT3000's explicit HVAC domain.

The fuel cell and its ancillary systems are represented with a component that is divided into three control volumes (shown schematically in Figure 1). The first control volume represents the FC, the fuel reformer (in the case of externally reforming systems), the fuel and air supply systems (including fans), and the power conditioning system that converts the electrical power from direct to alternating current. The second and third control volumes represent the exhaust-to-water heat exchanger: control volume two corresponds to the gas side of the heat exchanger while control volume three represents the water side.

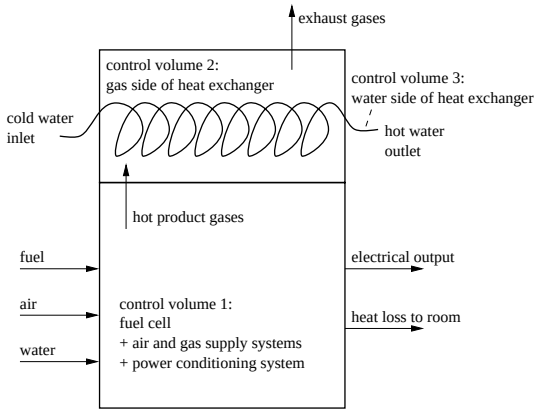

Figure 1: Fuel cell component model

A combination of empirical and first principle approaches are used to write the energy balances for the three control volumes. Molar mass balances determine the composition and properties of the hot product gases entering the heat exchanger while empirical relations in parametric form represent the fuel cell's thermal and electrical performance. This empirical approach is well suited to the current state and rapid pace of fuel cell development as the model makes direct use of benchmark test results.

Energy balance for first control volume

This approach is best illustrated by examining the energy balance for the first control volume. Starting with the general form (equation 1) the energy balance for this control volume can be represented by,

$$\sum_{i=1}^{fuel}(\dot{N}h)_i + \sum_{j=1}^{air}(\dot{N}h)_j + (\dot{N}h)_{water} + \phi_{chemical} \quad (2)$$

$$= q_{net-elec} + \sum_{k=1}^{products}(\dot{N}h)_k + q_{skin-losses}$$

A quasi steady-state modelling approach has been adopted. As such, the thermal transient term of equation 1 is not included in this energy balance. Each term of equation 2 is examined in turn.

Inlet streams

The first three terms in equation 2 represent the rate at which enthalpy is carried into the control volume by the fuel, air, and liquid water (optional) supplied to the fuel cell. $\dot{N}_i$ is the molar flow rate (kmol/s) of molecular constituent i and h_i is its molar enthalpy (J/kmol). The composition of the air and fuel streams is defined in terms of molar fractions. The composition of air is fixed while the user specifies the fuel mixture in terms of molar fractions of: hydrogen (H_2); the hydrocarbons methane (CH_4), ethane (C_2H_6), and propane (C_3H_8); and the non-combustibles carbon dioxide (CO_2) and nitrogen (N_2). In this way, the model can simulate fuel cell's supplied by pure hydrogen or by natural gas of any composition.

The enthalpy of each fuel and air constituent flowing into the control volume is then evaluated using a relation in the form of $h = f(T)$. These are derived from data given by Keenan et al (1980) and Jones and Hawkins (1960), and express the enthalpy relative to a common datum of 25^oC. The relation for CH_4, for example, is given by,

$$h_{CH_4} = [8.9 \cdot 10^5] + [3.5 \cdot 10^4] \cdot T + [26] \cdot T^2 \quad (3)$$

where T is in ^oC and h is in $J/kmol$. The fuel, air, and liquid water streams are assumed to enter the control volume at the temperature of the room containing the fuel cell.

The flow rate of liquid water introduced to the fuel cell is defined by the user as a function of the net electrical output (not presented here for the sake of brevity). The flow rates of the fuel and air streams

will be treated shortly.

Energy conversion

$\phi_{chemical}$ in equation 2 represents the rate at which the fuel's chemical energy is converted to electrical and thermal energy through electrochemical reactions (W),

$$\phi_{chemical} = \sum_{i=1}^{fuel} (\dot{N} \cdot LHV)_i = \dot{N}_{fuel} \cdot LHV_{fuel} \quad (4)$$

Where LHV_i is the lower heating value (J/kmol) of fuel constituent i. $\dot{N}_{fuel}$ is the total flow rate of all fuel constituents and LHV_{fuel} is the energy content expressed on a fuel molar basis: $LHV_{fuel} = \sum n_i \cdot LHV_i$, where n_i is the molar fraction of constituent i. Equation 4 is evaluated with the user-specified fuel molar fractions using tabulated LHV_i data (ASHRAE 2001).

Electrical efficiency

$q_{net-elec}$ in equation 2 is the net electrical output (W) from the fuel cell. This is equal to the cell output less the power consumption of fans, losses in the power conditioning system, and other system inefficiencies. The overall electrical conversion efficiency is defined as the ratio of the net electrical output to the rate at which chemical energy is supplied to the fuel cell,

$$\eta_E = \frac{q_{net-elec}}{\phi_{chemical}} \quad (5)$$

A parametric relation is used to express η_E as a function of the net electrical output,

$$\eta_E = \eta_0 + \eta_1 \cdot q_{net-elec} + \eta_2 \cdot q_{net-elec}^2 \quad (6)$$

The choice of the η_i coefficients (user inputs) determines the shape of the efficiency curve, which facilitates the use of empirical data, an important consideration in these early days of FC-cogeneration development. Data from benchmark testing of prototypes can be utilized immediately in modelling work simply by adjusting the η_i coefficients input to the simulation program. As knowledge of residential-scale FC systems develops, equation 6 could be replaced by a relation (or a complex algorithm) based upon first principle calculations.

Control of electrical output

ESP-r/HOT3000's building thermal domain determines the thermal demands placed upon the FC-cogeneration system on a time-step basis. In contrast, the electrical demands placed upon the FC-cogeneration system are user-specified. The user prepares a data-input file specifying the house's non-HVAC electrical demand at 5-minute intervals. This includes the total load generated by lighting, appliances, home entertainment, and other equipment. The demand imposed by HVAC equipment (pumps, fans, and compressors) is calculated during the simulation. Although this approach requires significant data input (105 120 non-HVAC data points for an annual simulation) the format is structured to simplify the generation of these input files using pre-processors such as spreadsheet programs.

At each time-step of the simulation the non-HVAC electrical load is read from the data input file and the fuel cell controlled to respond to this demand. Three control strategies currently exist to determine $q_{net-elec}$. The fuel cell can provide a constant output or its output can modulate in response to the house's electrical demand (electrical priority). With the third control strategy, the fuel cell is operated in an attempt to minimize the energy required for supplementary space and DHW water heating (thermal priority). The model has been structured to facilitate the inclusion of additional control strategies in the future.

Fuel consumption

Once $q_{net-elec}$ is established for the current time-step, equations 4 to 6 are combined to solve for the rate of fuel consumption,

$$\dot{N}_{fuel} = \frac{q_{net-elec}}{LHV_{fuel} \cdot \left[\eta_0 + \eta_1 \cdot q_{net-elec} + \eta_2 \cdot q_{net-elec}^2\right]} \quad (7)$$

The consumption rates of the individual fuel constituents ($\dot{N}_i$) are derived for equation 2 using the solution of equation 7 and the fuel's molar fractions.

Air supply

The air supplied to the control volume is governed by system design variables: the supply fan flow characteristics, ductwork, and fan control strategies. This dictates an empirical modelling approach. As such, a parametric relation is used to express the air flow as a function of the net electrical output,

$$\dot{N}_{air} = w_0 + w_1 \cdot q_{net-elec} + w_2 \cdot q_{net-elec}^2 \quad (8)$$

Again, data from benchmark testing of prototypes can be utilized immediately in modelling work simply by adjusting the w_i coefficients input to the simulation program. The flow rates of the individual air constituents ($\dot{N}_j$) required for equation 2 are derived from the solution of equation 8 and the (fixed) composition of the air.

Product gases

The second term on the right side of equation 2 represent the rate at which enthalpy is carried out of the control volume by the gases which are produced by the reforming and electrochemical reactions. Complete reactions are assumed[1]. Given this, the net

[1] A reasonable assumption for externally reforming fuel cells and the high-temperature SOFCs.

chemical reactions occurring between the control volume's inlets and outlet are given by,

$$H_2 + \tfrac{1}{2} O_2 \rightarrow H_2O \quad (9)$$

$$CH_4 + 2O_2 \rightarrow CO_2 + 2H_2O$$

$$C_2H_6 + \tfrac{7}{2} O_2 \rightarrow 2CO_2 + 3H_2O$$

$$C_3H_8 + 5O_2 \rightarrow 3CO_2 + 4H_2O$$

The user-specified fuel composition and equation 7 determine the hydrogen and hydrocarbon flow rates for equation 9. This also determines the flow rate of CO_2 introduced with the fuel. The air composition and equation 8 determines the O_2, CO_2, and H_2O added to the control volume from the air stream. Given this, equation 9 is solved to determine the flow rates of O_2, CO_2, and H_2O leaving the control volume. The gas mixture exiting the control volume also contains N_2 and Ar, but as these are inert the quantity in the products is equal to the quantity carried in by the air and fuel streams[2].

Once the composition and flow rate are established, the enthalpies of the products exiting the control volume are determined. The enthalpy of each gas in the product stream is evaluated using $h = f(T)$ relations in the form of equation 3.

ESP-r/HOT3000's explicit HVAC domain solves the state point of each control volume in terms of temperature. Therefore, the temperature of the product gases is introduced into the energy balance by recognizing that $c_p \equiv (\partial h/\partial T)_P$. With this, the second term on the right side of equation 2 is expressed as,

$$\sum_{k=1}^{products} (\dot{N} h)_k = \quad (10)$$

$$\sum_{k=1}^{products} \dot{N}_k \cdot \left[c_p (T_{products} - T_{ref}) + h_{T_{ref}} \right]_k$$

T_{ref} is a reference temperature used to evaluate the $(\partial h/\partial T)_P$ derivative and $h_{T_{ref}}$ is the relative enthalpy of the product gas constituent at this reference temperature. As the enthalpies of the product gases are fairly linear with temperature, this provides great flexibility in selecting T_{ref}. A value of -100^oC was selected upon conducting a sensitivity study as this value avoids any possibility of numerical instability.

Heat loss to room

The final term in equation 2, $q_{skin-losses}$, represents the heat lost to the room containing the fuel cell. In the current model this is treated as a constant (user-specified) value. This will be replaced with a more detailed treatment once sufficient information on system configurations is established.

This completes the evaluation of the energy balance for the first control volume. Processing of the equation will be discussed following an examination of the energy balances for the two other control volumes.

Energy balance for second control volume

The energy balance for the second control volume (the gas side of the heat exchanger) is given by,

$$\sum_{k=1}^{products} (\dot{N} h)_k = \sum_{l=1}^{exhaust} (\dot{N} h)_l + q_{heat-recovery} \quad (11)$$

The left side of equation 11 represents the rate at which enthalpy is carried into the control volume by the product gases exiting the first control volume. The first term on the right side is the rate at which enthalpy leaves the control volume through the rejection of the cool exhaust. As no chemical reactions occur within the heat exchanger, the flow rate of each exhaust gas is equal to the flow rate of each product gas (ie. $\dot{N}_l = \dot{N}_k$). The enthalpy of the gas constituents is treated as before and the temperatures of the exhaust ($T_{exhaust}$) and product gases ($T_{products}$) are introduced into equation 11 using the technique elaborated for the first control volume.

The last term in equation 11 represents the thermal energy transferred to the water, that is the FC-cogeneration's thermal output. This is evaluated using the approach temperature and an effective heat transfer coefficient,

$$q_{heat-recovery} = UA_{eff} \cdot (T_{products} - T_{water,in}) \quad (12)$$

Where $T_{water,in}$ is the temperature of the water entering the heat exchanger (^oC).

A parametric relation is used to establish the effective heat transfer coefficient,

$$UA_{eff} = q_0 + q_1 \cdot \left(\sum_{k=1}^{products} \dot{N}_k \right) + q_2 \cdot \left(\sum_{k=1}^{products} \dot{N}_k \right)^2 \quad (13)$$

The form of equations 12 and 13 allow the heat recovery to vary in response to the temperature and flow rate of the hot product gases. As with the electrical efficiency and air supply relations, data from benchmark testing of the heat exchanger at the relevant flow rates and temperatures can be reflected immediately through the selection of the q_i coefficients that are input to the simulation program.

Energy balance for third control volume

The energy balance for the third control volume (the water side of the heat exchanger) is given by,

[2] Some NO_x is also produced, but the quantities are insignificant.

$$q_{heat-recovery} = \dot{m}(h_{water,out} - h_{water,in}) \quad (14)$$

Where $\dot{m}$ is the mass flow rate (kg/s) of water through the heat exchanger. As the heat capacity of water, $c_{p,water}$, varies only weakly over the heat exchanger's range of operating temperatures, equation 14 can be expressed as,

$$q_{heat-recovery} = \dot{m} c_p (T_{water,out} - T_{water,in}) \quad (15)$$

Matrix of energy balance equations

With the approach elaborated above, the energy balances for the three control volumes can be organized into a matrix of the following form,

$$\begin{bmatrix} a_{1,1} & & & \\ a_{2,1} & a_{2,2} & & \\ a_{3,1} & & a_{3,3} & a_{3,4} \end{bmatrix} \times \begin{bmatrix} T_{products} \\ T_{exhaust} \\ T_{water,out} \\ T_{water,in} \end{bmatrix} = \begin{bmatrix} z_1 \\ z_2 \\ z_3 \end{bmatrix} \quad (16)$$

The first row of the matrix is the energy balance for the control volume representing the fuel cell and its ancillaries (equations 2). The second and third rows represent the energy balances for the heat exchanger (equations 11 and 15). The $a_{i,j}$ coefficients are derived by evaluating and combining the individual terms of the energy balances. For example, $a_{1,1}$ modifies $T_{products}$ in the first energy balance and is evaluated using equation 10.

The temperature vector represents the variables whose solution is sought. The first three temperatures ($T_{products}$, $T_{exhaust}$, and $T_{water,out}$) represent the thermal state of the fuel cell component while the fourth temperature ($T_{water,in}$) represents the state of a connected component (the pipe delivering water to the heat exchanger). The z coefficients represent quantities not dependent upon the temperatures of the control volumes. z_1, for example, contains terms derived from equations 3, 4, 7, and 8.

A matrix in the form of equation 16 is formed for each component in the HVAC plant network representing the FC-cogeneration system (water storage tanks, pumps, pipes, etc.). Some of these other matrices contain coupling terms to the fuel cell matrix. For example, the matrix representing the pipe that delivers hot water from the fuel cell heat exchanger to a water storage tank would contain a term modifying $T_{water,out}$. These component matrices are assembled into a global matrix and solved using the direct-iterative technique (including handshaking with the building thermal domain) that was described earlier.

APPLICATION

Application of the new model for simulating SOFC-cogeneration systems is demonstrated in this section.

An HVAC plant network is formed by combining the SOFC model with component models for a gas-fired water storage tank (also developed for this project), pumps, fans, and pipes. The thermal output of the SOFC is transferred to the water storage tank. This tank directly supplies the house's DHW needs while space heating requirements are met through a fan-coil system connected to the water tank. A pump circulates water from the storage tank to the SOFC's heat exchanger while a second pump circulates hot water from the storage tank to the fan-coil unit.

The tank's natural gas burner cycles on when the tank temperature drops below its set-point (50^oC in this case). As such, the burner only consumes gas when the SOFC's thermal output is insufficient to meet the houses' space heating and DHW requirements. A safety device is modelled by extracting hot water from the tank when its temperature rises above a safety limit (65^oC in this case). When the SOFC's thermal output exceeds the house's space heating and DHW requirements and exceeds the tank's ability to store this energy, this safety device essentially dumps the SOFC's excess thermal output.

The coefficients defining the SOFC's performance characteristics (for equations 6, 8, and 13) correspond to the system under development at FCT. The HVAC network representing this SOFC-cogeneration system was connected to a model of a modern energy-efficient house (meeting the R-2000 standard) of typical dimensions and located in Montréal. The DHW draw schedule and house's non-HVAC electrical loads were selected to be typical of a family of four. An annual simulation was performed with the SOFC model's electrical priority controller using 5-minute time-steps.

Some aspects of the SOFC's performance are illustrated in Figure 2. This plot compares the product and exhaust gas temperatures over the full simulation period as well as contrasting the SOFC's thermal and electrical output. As can be seen, the temperature of the product gases entering the heat exchanger is between 300^oC and 400^oC over most of the SOFC's operating range while the temperature of the exhaust gases exiting the heat exchanger range from 100^oC to 200^oC. The average temperature drop of the gases through the heat exchanger is 185^oC.

Figure 2 illustrates that the $q_{heat-recovery}/q_{net-elec}$ ratio is 65% to 75% at the lower end of the SOFC's operating range. Due to the impact of the product gas flow rate on the heat exchanger (refer to equation 13), it is as high as 91% at the SOFC's upper operating limit. The average $q_{heat-recovery}/q_{net-elec}$ ratio over the annual simulation is 73%.

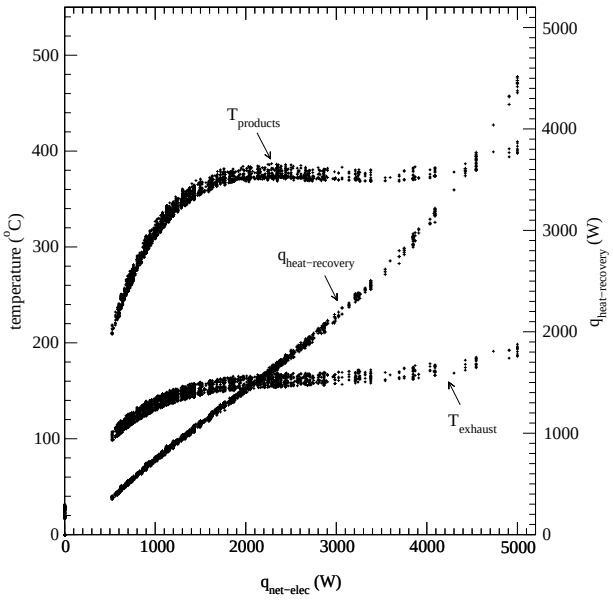

Figure 2: SOFC product and exhaust gas temperatures and thermal output

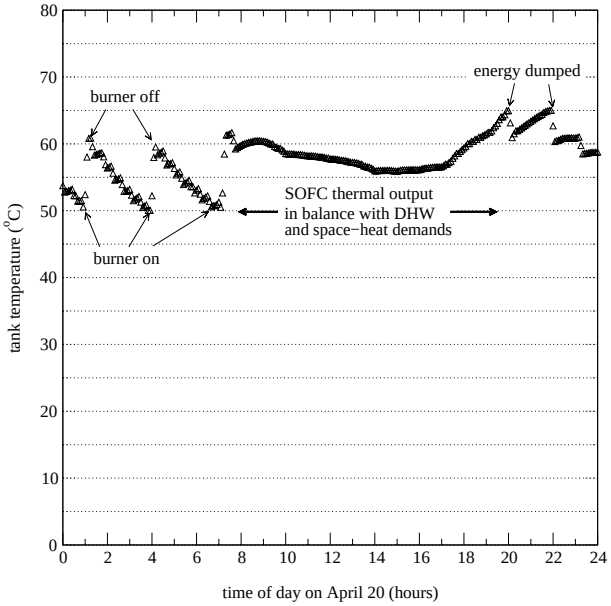

Figure 3: Temperature of water in storage tank

The thermal state of the water tank is illustrated in Figure 3. This plots the tank temperature over a typical day in April. The various operational states are clearly seen in this figure. The tank's burner cycles on whenever the water temperature drops below 50^oC and stays on until the upper limit of the burner's set-point (60^oC in this case) is achieved. The tank is seen to cool down between burner shut-off and turn-on as the tank is cooled due to DHW and space-heating draws. The burner cycles on three times from midnight to about 7h00, illustrating that during this period the SOFC's thermal output cannot fully respond to the house's demands. The burner does not cycle on from 7h00 to 18h00 and the tank's temperature remains within the range of the burner's set-points. During this period the SOFC's thermal output is in equilibrium with the DHW and space-heating demands. However, the tank temperature rises after 18h00 and at 20h00 it reaches the safety limit of 65^oC. Energy is dumped at this point, but the tank overheats again at 22h00. During this period much of the SOFC's thermal output cannot be exploited by the house and this energy is essentially wasted.

The overall thermal energy balance of the SOFC-cogeneration system is illustrated in Figure 4. This plots the monthly integrated energy inputs to the water tank as well as the energy dumped through the tank's safety device. As can be seen, the SOFC's thermal output is nearly constant over the year. This result is consistent with the control scheme (electrical priority) selected for this simulation. Significant energy is added by the burner during the heating season, but the burner is inactive from May through September when the heating system is shut off. The only draws on the tank during this period are for DHW. Therefore, during these months the SOFC's thermal output is sufficient to meet all DHW requirements. Figure 4 shows that the safety device is activated frequently when the heating system is shut off as well as in the swing months of April and October when space heating requirements are minimal.

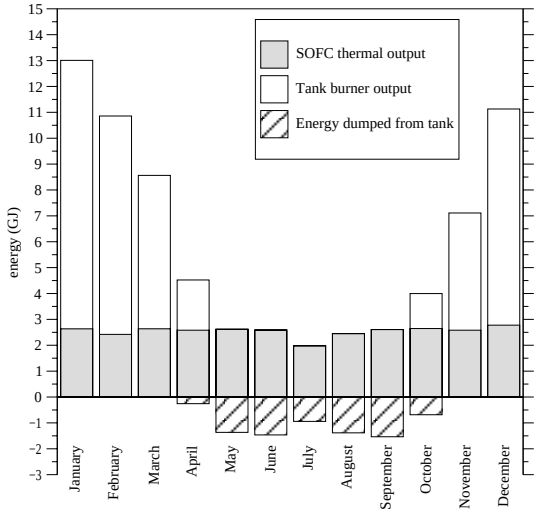

Figure 4: Monthly energy balance on water tank

The SOFC delivers 30.5 GJ of thermal energy to the water tank over the year. However, 7.6 GJ of this energy is rejected by the safety device to prevent overheating in the tank. Therefore, the SOFC's net

thermal contribution is 22.9 GJ. The tank burner delivers 40.9 GJ of energy to supplement the SOFC's output. Therefore for this specific case, the SOFC meets 36% of the house's total thermal requirements.

The SOFC responds to 99% of the house's electrical demands, delivering 11 608$kWhr$ (41.8 GJ) of electrical energy over the year. It consumes 2 640m^3 of natural gas to produce its electrical and thermal output. Therefore, the total (electrical plus thermal) efficiency of the SOFC-cogeneration system expressed in terms of the fuel's LHV[3] for this case is determined by,

$$\eta_{cogen} = \frac{(41.8 + 22.9)GJ}{(0.0359GJ/m^3) \cdot (2\,640m^3)} = 68\% \qquad (17)$$

CONCLUSIONS

Fuel cells are an interesting technology for residential-building scale DG because they offer the potential for cogeneration—the concurrent production of electrical and thermal energy. However, whether a fuel cell's thermal output can be effectively exploited within a house is a complex question to answer. The interaction between a house's thermal and electrical performance and an FC-cogeneration unit represents a complex thermodynamic system. Furthermore, the factors which affect the performance are numerous, such as: the occupants' electrical and domestic hot water usage patterns; the house's thermal characteristics; weather; the fuel cell's performance characteristics and operational strategies; and the configuration, design, and operation of the other HVAC components.

The complex nature of this problem is well suited to simulation. To this end a fuel cell model was developed within the ESP-r/HOT3000 program. This model is useful for analyzing the technical and economic potential of FC-cogeneration systems and as an R&D tool for assessing and optimizing system design variants. Empirical relations in parametric form are used to represent the fuel cell's thermal and electrical performance whereas mass balances and thermodynamic relations are used to determine the temperature and flow rate of hot product gases entering the cogeneration unit's exhaust-to-water heat exchanger. This approach is well suited to the current state and rapid pace of fuel cell development as the model makes direct use of benchmark test results.

The new model is demonstrated by simulating a modern energy-efficient house serviced by an SOFC-cogeneration system. The house is located in Montréal and its DHW and electrical usage patterns are typical of a family of four. The SOFC-cogeneration's thermal output is found to be sufficient to meet all DHW requirements from May through September and to contribute significantly to the house's space heating in the winter and swing seasons. Over the full year, the SOFC meets 99% of the house's electrical demands and 36% of the house's thermal requirements. The total (electrical plus thermal) efficiency of the SOFC-cogeneration system expressed in terms of the fuel's LHV is found to be 68%. This result is particularly impressive as no attempt was made to optimze the system configuration to match the house's requirements. Further simulations could be performed to help tune the system's output to match the house's requirements, thus leading to a higher total efficiency. It is also important to underline that these results cannot be generalised, but rather are limited to the specific case simulated.

Although the new fuel cell model represents a step forward in the modelling of residential DG-cogeneration systems, there is much room for refinement. Future enhancements and additions to the model are planned, such as the modelling of thermal cooling, consideration of the fuel cell's thermal and electrical transients, and more detailed treatment of DHW and electrical demands. Extensive validation of the model for SOFC and other cogeneration systems is also planned for the future.

[3] The LHV for the natural gas composition used in this simulation is 35.9 MJ/m^3.

REFERENCES

ASHRAE (2001), *Fundamentals*, SI Edition, American Society of Heating, Refrigerating and Air-Conditioning Engineers Inc, Atlanta USA.

Clarke J.A. (2001a), *Energy Simulation in Building Design*, (2nd Edn), Butterworth Heinemann.

Clarke J.A. (2001b), 'Domain Integration in Building Simulation', *Energy and Buildings*, 33 303-308.

Ellis M.W. and Gunes M.B. (2002), 'Status of Fuel Cell Systems for Combined Heat and Power Applications in Buildings', *ASHRAE Transactions*, AC-02-18-2.

ESRU (2000), *The ESP-r System for Building Energy Simulations: User Guide Version 9 Series*, ESRU Manual U00/1, University of Strathclyde, Glasgow UK.

Hensen J.L.M. (1991), *On the Thermal Interaction of Building Structure and Heating and Ventilation System*, PhD Thesis, Eindhoven University of Technology, The Netherlands.

Jones J.B. and Hawkins G.H. (1960), *Engineering Thermodynamics*, John Wiley & Sons.

Keenan J.H., Chao J., and Kaye J. (1980), *Gas Tables*, John Wiley & Sons.

US-DOE (2000), *Fuel Cell Handbook*, 5th Edn, United States Department of Energy, Morgantown.